

Expanding Bubbles in a Thermal Background

Richard M. Haas*

Department of Physics, University of Florida, Gainesville, FL 32611
(UFIFT-HEP-97-9 January 1998)

Real scalar field models incorporating asymmetric double well potentials will decay to the state of lowest energy. While the eventual nature of the system can be discerned, the determination of the dynamics of the bubble wall provides many difficulties. In the present study we investigate numerically the evolution of spherically symmetric expanding bubbles coupled to a thermal bath in $3 + 1$ dimensions. A Markovian Langevin equation is employed to describe the interaction between bubble and bath. We find the shape and velocity of the wall to be independent of temperature, yet extremely sensitive to both asymmetry and viscosity.

PACS: 11.10.Lm, 05.70.Lm, 98.80.Cq

I. INTRODUCTION

The behavior of fields during weak first order phase transitions has been a source of great interest. Several studies have shown either a need for changes to the current theory of thermal phase transitions or the inclusion of carefully calculated corollaries to the present models [1–3]. Sub-critical bubbles and oscillon solutions may give rise to phase mixing in which these fluctuations in the smooth homogeneous background can have significant dynamical effects. Thus in the limit of weak first order phase transitions, the assumption of small amplitude fluctuations may need revision. For stronger transitions, the fluctuations are expected to diminish in importance validating the use of standard homogeneous nucleation theory. Yet, in the realm of the expanding bubble, precious few analytic and numerical studies have been performed to determine the effect of the thermal bath on the expansion of the bubbles [4,5]. With this in mind, we numerically examine expanding bubbles in $3 + 1$ dimensions using a Langevin equation in hopes of gaining either qualitative or quantitative results that describe their behavior.

Symmetry restoration at various stages in the Universe's life has become an important and powerful concept in modern cosmology. Several examples of the relevance of phase transitions are given by inflation [6], the electroweak phase transition [7], and the quark hadron phase transition [8]. In particular, the phase transition that occurred when the universe cooled to a critical tem-

perature of about 300 GeV broke the symmetry of the weak and electromagnetic interactions. The breakdown of $SU(2) \times U(1)$ which may have created the baryon asymmetry we see today is expected to be of first order [9]. This satisfies the third of Sakharov's conditions for baryogenesis, namely that no thermal equilibrium exist [10].

At the electroweak scale, the rate of expansion of the universe is such that thermal equilibrium is maintained [11]. To create an out of equilibrium process, a bubble of true vacuum appears within the false vacuum state. As the bubble expands, baryogenesis takes place in the neighborhood of the boundary of the bubble, the bubble wall. Thus, the detailed behavior of the bubble wall is of great importance in the electroweak phase transition.

The nucleation of bubbles in the context of field theory has by now a long history. Coleman has shown that at zero temperature, the transition to the true vacuum takes place via the quantum nucleation of bubbles [12]. This process corresponds to a generalization of barrier penetration in quantum mechanics. The probability for bubble nucleation at zero temperature is found by determining the “bounce” configuration from the Euclidean equation of motion subject to the boundary conditions of restricting the field to the metastable minimum at $t_E = -\infty$, the global minimum at $t_E = 0$, and the metastable minimum at $t_E = +\infty$. The bounce solution is used to compute the Euclidean action, from which bubble nucleation probability per unit volume is determined, $\Gamma = A \exp(-S_E)$. The dominant contribution to

*email: rhaas@phys.ufl.edu

the tunneling rate comes from the solution to the equation of motion with the least action. These solutions are $O(4)$ symmetric, satisfying a $O(4)$ symmetric Euclidean equation of motion. The nucleating bubbles were shown to quickly accelerate to the speed of light.

Linde expanded Coleman's ideas to account for finite-temperature effects in the nucleation of bubbles [13]. Temperature effects can be included by formal substitution of the Euclidean time to include temperature, imposition of periodic boundary conditions on the field, and integration in the "new" Euclidean time from 0 to 1 [14]. For high temperatures, the kinetic term in the action grows large. Yet, as solutions which minimize the action are sought, the time independent configurations will dominate. The $O(3)$ Euclidean equation can be solved to find the finite temperature bounce. The rate of thermal nucleation of critical bubbles per unit volume was found to include an "activation energy" term representing the free energy barrier the system must overcome for the transition to occur. The thermal fluctuations were shown to be a purely classical effect. Thus the previous results of the bounce solutions also apply to the finite-temperature case with different configurations for different temperatures.

Recent numerical studies have shown that the actual first order phase transition from false to true vacuum in the presence of a heat bath may be a great deal more complicated than indicated from the picture of a finite temperature bounce solution. For weak first order phase transitions, phase mixing through sub-critical bubbles may effectively restore the symmetry [1]. Long-lived sub-critical bubbles, oscillons, may act as nucleation sites for critical bubbles, thus speeding the transition rate [2,3]. Although the importance of these effects are still somewhat in dispute [15], it is clear that significant deviations from the standard model of bubble nucleation may occur and that carefully considered numerical calculations must be performed in order to determine the behavior of the system.

Previous studies of thermal nucleation of bubbles have dealt with systems in lower dimensions. Work in 1+1 dimensions has primarily focused on the nucleation of kink-antikink pairs [16]. The behavior that was examined was the kink density and lifetime for a wide range of viscosities and temperatures. The numerical results showed good agreement with the theoretical expectations. In 2+1 dimensions, studies have focused on the validity of theoretical calculation of the nucleation barrier when compared to numerical results [17] and the effect of fluctuations on the structure and velocity of the expanding bubble wall [5].

In this study, we will investigate the behavior of a 3+1 dimensional bubble expanding in a thermal background. To insure uncontaminated results, the field is localized in the metastable vacuum with the heat bath acting until a bubble is formed. Although this requires longer compu-

tational times, it provides results which occur naturally from the equations of motion without need for an artificial contrivance. We hope to shed light on two vital characteristics of the transition from our study as the asymmetry of the potential, the bath's viscosity, and the bath's temperature are changed: 1. the shape of the bubble wall, and, 2. the speed at which the bubble wall travels.

The rest of this work is organized as follows. In the next section, we briefly review the properties that give rise to expanding bubbles and the bounce solutions found by Coleman [12]. In Section III, we discuss the effects of coupling the system to a thermal bath by generalizing the equation of motion found in section II using a Langevin form. In Section IV, we present the numerical results. In Section V, we summarize our results, pointing to possible directions for future work.

II. EXPANDING BUBBLES

The behavior of a real scalar field follows from the form of the action,

$$S = \int d^4x \left[\frac{1}{2} (\partial_\mu \phi)^2 - V(\phi) \right]. \quad (1)$$

Through use of Hamilton's principle, the classical equation of motion for the field is found to be

$$\frac{\partial^2 \phi}{\partial t^2} - \nabla^2 \phi = - \frac{\partial V(\phi)}{\partial \phi}. \quad (2)$$

To determine the energy of the field, we integrate in space over the stress-energy tensor,

$$E(\phi) = \int d^3x T^{00} = \int d^3x \left[\frac{1}{2} (\dot{\phi})^2 + \frac{1}{2} (\nabla \phi)^2 + V(\phi) \right] \quad (3)$$

where the dot refers to partial differentiation with respect to time. Thus, by specifying the potential, we will obtain an explicit equation of motion for the system and a determination of the energy of the field.

In the early universe, and, particularly, in the case of the electroweak phase transition, the approximate expression for the effective potential in the high temperature limit to one loop order is [18]

$$V(\phi, T) = D(T^2 - T_0^2)\phi^2 - ET\phi^3 + \frac{\lambda_T}{4}\phi^4 \quad (4)$$

where

$$D = \frac{1}{8v_0^2} (2m_W^2 + m_Z^2 + 2m_t^2)$$

$$E = \frac{1}{4\pi v_0^3} (2m_W^3 + m_Z^3) \sim 10^{-2}$$

$$T_0^2 = \frac{1}{2D} (\mu^2 - 4Bv_0^2)$$

$$\lambda_T = \lambda - \frac{3}{16\pi^2 v_0^4} \left(2m_W^4 \ln \frac{m_W^2}{a_B T^2} + m_Z^4 \ln \frac{m_Z^2}{a_B T^2} - 4m_t^4 \ln \frac{m_t^2}{a_F T^2} \right)$$

To solve the equation of motion for our system, we introduce three boundary conditions. The field initial starts at rest,

and $2\mu^2 = m_H^2$, $\ln a_B = 2 \ln 4\pi - 2\gamma \simeq 3.91$, $\ln a_F = 2 \ln \pi - 2\gamma \simeq 1.14$. Analyzing the temperature dependence of equation 4, we find that for large temperatures the potential exhibits a single unique minimum at $\phi = 0$. As the system evolves and cools, a non-global second minimum forms at a temperature of

$$T_1 = \frac{T_0}{\sqrt{1 - 9E^2/8\lambda_{T_1} D}}.$$

With further cooling, degenerate minima of the potential form at the critical temperature T_c given by

$$T_c = \frac{T_0}{\sqrt{1 - E^2/\lambda_{T_c} D}}.$$

The minima are located at

$$\phi = 0 \quad \text{and} \quad \phi_c = \frac{2ET_c}{\lambda_{T_c}}.$$

When $T < T_c$ a new global minimum is formed. At $T = T_0$, the potential's global minimum is located at

$$\phi = \frac{3ET_0}{\lambda_{T_0}}$$

For $T < T_c$, first order phase transitions are possible for the system described by $V(\phi, T)$. The cubic term in the potential is responsible for barrier formation and the asymmetry between stable and metastable states. The strength of the asymmetry depends upon ET . To simplify the expression for equation 4 while retaining the parameters of physical interest and allow for possible applicability to other similar first order scenarios, the potential is written as

$$V(\phi) = \frac{m^2}{2}\phi^2 - \frac{\alpha m}{3}\phi^3 + \frac{\lambda}{4}\phi^4. \quad (5)$$

The variable α will be a measure of the asymmetry between the two minima.

To cast the system into a more tractable form, two further steps can be taken to simplify the equation of motion. By imposing spherical symmetry, we effectively reduce this problem to one dimension. This allows for quicker computational manipulation and a clearer understanding of what is driving the system's behavior. By neglecting azimuthal and longitudinal components, this study will serve to provide bounds on the behavior of the expanding bubble. Introducing the dimensionless variables $\rho = rm$, $\tau = tm$, $\Phi = \frac{\sqrt{\lambda}}{m}\phi$, and $\tilde{\alpha} = \frac{\alpha}{\sqrt{\lambda}}$ the nonlinear equation of motion becomes

$$\frac{\partial^2 \Phi}{\partial \tau^2} - \frac{\partial^2 \Phi}{\partial \rho^2} - \frac{2}{\rho} \frac{\partial \Phi}{\partial \rho} = -\Phi + \tilde{\alpha} \Phi^2 - \Phi^3. \quad (6)$$

$$\dot{\Phi}(\rho, 0) = 0.$$

To avoid an undefined value at the origin, the spatial derivative is fixed

$$\frac{d\Phi(0, \tau)}{d\rho} = 0.$$

Eventually the system will nucleate a bubble of true phase in the false one. Thus, at spatial infinity we expect the field to be in the false vacuum state,

$$\Phi(\rho \rightarrow \infty, \tau) = \Phi_0.$$

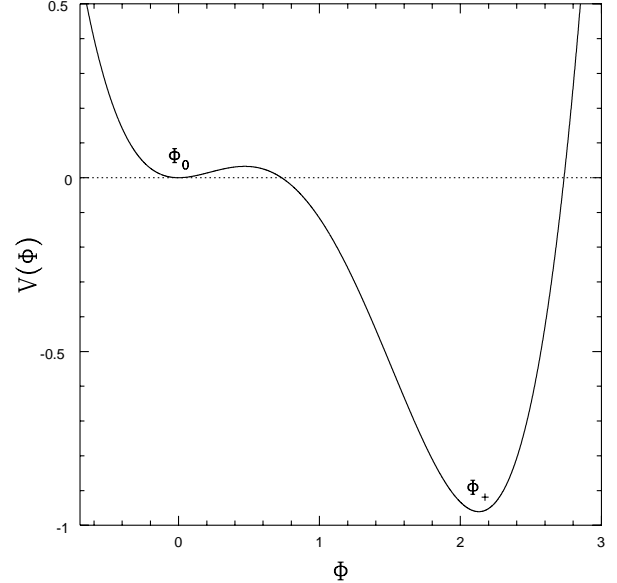


FIG. 1. Asymmetric double well potential with $\tilde{\alpha} = 2.6$.

Using the dimensionless variables, the characteristics of the potential can be determined. The minima of the potential are at

$$\Phi = 0 \quad \text{and} \quad \Phi_+ = \frac{\tilde{\alpha}}{2} \left[1 + \left(1 - \frac{4}{\tilde{\alpha}^2} \right)^{\frac{1}{2}} \right].$$

For $\tilde{\alpha} = \sqrt{\frac{9}{2}}$, the potential is degenerate. As shown in figure 1, when $\tilde{\alpha} > \sqrt{\frac{9}{2}}$, Φ_+ becomes the stable vacuum and the possibility for the creation of expanding bubbles exists. The classical turning point of the potential is found at

$$\Phi_{tp} = \frac{2}{3} \tilde{\alpha} \left[1 - \left(1 - \frac{9}{2\tilde{\alpha}^2} \right)^{\frac{1}{2}} \right]. \quad (7)$$

The zero temperature bounce [12] and the finite temperature bounce [13] solutions are needed in calculating the bubble nucleation rate. To calculate the bounce, we write a Euclidean version of equation 2 through use of $t \rightarrow -ix^0$ and $x^2 = t^2 - |\mathbf{x}|^2 \rightarrow -(x^0)^2 - |\mathbf{x}|^2 = -|x_E|^2$. The boundary conditions restrict the field to be localized in one of the minima of the asymmetric double well potential at $x^0 = \pm\infty$, hence the name “bounce”. The least action Euclidean solution will contribute most to the nucleation rate, having $O(4)$ symmetry. Recalling that a connection between the path integral formulation of quantum field theory and the statistical mechanics partition function can be found by the formal substitution of $x^0 \rightarrow \beta$ with $\beta = \frac{1}{kT}$, defining the functions on a domain of length β and periodically connected in time, the finite temperature action can be determined. The functional integral for the action now contains a kinetic term of quadratic order in temperature. At high temperature, this term can be neglected as we are looking for the solution which minimizes the action. In other words, the least action solution in finite temperature will be time-independent and have $O(3)$ symmetry. The $O(3)$ spherically symmetric equation of motion is

$$\frac{d^2\Phi}{d\rho^2} + \frac{2}{\rho} \frac{d\Phi}{d\rho} = \frac{\partial V(\Phi)}{\partial \Phi}. \quad (8)$$

For the asymmetric double well potential, no closed-form solution exists to equation 8. However, approximate solutions can be determined if one restricts the investigation to asymmetries that are small compared to the barrier height of the potential. For the dimensionless form of the potential this amounts to $\tilde{\alpha} \rightarrow \sqrt{\frac{9}{2}}$. In this limit, the volume energy dominates the surface energy in equation 3 only when the radii of the bubbles are large. Additionally, the transition between the vacua in $\Phi(\rho)$ occurs only in a small interval, thus giving rise to the name “thin-wall” approximation [12]. As the first order derivative term in equation 8 is only appreciable in a small transition region and ρ is large, we may approximate our equation of motion by

$$\frac{\partial^2\Phi}{\partial\rho^2} = \Phi - \tilde{\alpha}\Phi^2 + \Phi^3. \quad (9)$$

Solving this equation for $\Phi(\rho)$ we obtain the shape of the bubble in the thin-wall limit

$$\Phi = \frac{1}{\sqrt{2}} \left[1 - \tanh \left(\frac{\rho - R}{2} \right) \right], \quad (10)$$

with R the bubble radius. This solution will be of use later in our investigation when we compare the numerically generated bubble wall to the shape expected from a slightly asymmetric double well potential.

III. BOILING BUBBLES

To include the effects of a thermal background on the evolution of the field, a generalized Langevin equation can be formulated and solved numerically. Employing an analogy between classical Brownian motion and quantum field theory, we find an equation of motion by adding a viscosity and a noise term to our original equation of motion, equation 2. Assuming a Markovian heat bath, the viscosity coefficient is related to the noise $\xi(\mathbf{x}, t)$ by the fluctuation-dissipation theorem

$$\langle \xi(\mathbf{x}, t) \xi(\mathbf{x}', t') \rangle = 2\gamma T \delta(t - t') \delta^3(\mathbf{x} - \mathbf{x}'). \quad (11)$$

The coupling constants in this system are treated as free parameters. Although more complicated nonlocal forms of the Langevin equation could be used [19], the increased complexity in both the equation of motion and the dynamics do not warrant such an approach until the present situation is better understood. Indeed, the agreement between numerical studies and theoretical predictions of nucleation in 1+1 dimensions lends support to the use of an additive noise and a Markovian bath [16].

The system is restricted to spherical symmetry. As the thermal bath is provided with no symmetries, the proper evaluation of the system should contain all spatial dimensions. Yet the advantages provided by evaluating the fully dimensional case is questionable in light of the adversity this would cause. The computer simulations of a non-symmetric system would be expected to have significantly longer run times. More importantly, the dominant perturbations due to the thermal fluctuations are expected to be along the radial direction. By allowing only variations in the radial direction, a clearly defined bubble wall velocity can be determined. For these reasons, the values obtained here should be considered as an approximate bound on the velocities of expanding (3+1)-dimensional bubbles. Writing the fluctuation-dissipation theorem in terms of spherical symmetry, we obtain

$$\langle \tilde{\xi}(\rho, \tau) \tilde{\xi}(\rho', \tau') \rangle = \frac{1}{2\pi\rho^2} \tilde{\gamma} \theta \delta(\tau - \tau') \delta(\rho - \rho'), \quad (12)$$

where $\theta = \frac{\lambda}{m} T$ is the dimensionless temperature. The spherically symmetric dimensionless Langevin equation is written as

$$\frac{\partial^2\Phi}{\partial\tau^2} + \tilde{\gamma} \frac{\partial\Phi}{\partial\tau} - \frac{\partial^2\Phi}{\partial\rho^2} - \frac{2}{\rho} \frac{\partial\Phi}{\partial\rho} = -\Phi + \tilde{\alpha}\Phi^2 - \Phi^3 + \tilde{\xi}, \quad (13)$$

where $\tilde{\gamma} = \frac{\gamma}{m}$ and $\tilde{\xi} = \frac{\sqrt{\lambda}}{m^{\frac{3}{2}}} \xi$ are the dimensionless viscosity and noise respectively.

Equation 13 is numerically solved by a finite difference routine second order accurate in time and fourth order accurate in space. The step sizes employed in the simulation were determined rather crudely by specifying a numerically obtained bounce solution as the initial field configuration in the $\tilde{\gamma} = 0$ case and ensuring that this system behaved as expected for a sufficiently long time ($\tau > 6000$). Satisfactory results were found in these situations if a spatial step of $\delta_\rho = 10^{-2}$ and a temporal step of $\delta_\tau = 2 \times 10^{-3}$ were used.

The validity of equations 12 and 13 can be tested by comparing numerical results and theoretical predictions for the system subject to a quadratic potential. Given sufficient time, the thermal evolution of the field in the potential will reach equilibrium. Since the system is described by a spatial one dimensional lattice of N grid points, we can measure the energy per degree of freedom E/N . From basic statistical mechanics, we know that once the system is in equilibrium the equipartition theorem will give $E/N = \theta/2$. The numerical results for this situation do show that the equipartition theorem holds for our system over a wide range of parameters [See Figure 2 of Ref. [3]].

While we have explicitly formulated a system whose dynamics are given by the Langevin equation, many hydrodynamical studies have shed light upon the phase transition [20–22]. Whereas in the Langevin description the particles scattering off the bubble wall provide a damping proportional to the field’s change in time, a hydrodynamic description treats the wall as a combustion front. The results of the hydrodynamic work have shown various characteristics of expansion which are not manifest using the Langevin equation. Instabilities have been found in the background fluid and the bubble wall which may dominate the dynamics [21]. The velocity of the bubble wall has also been found to be dependent upon the thermal conductivity of the background fluid and upon temperature inhomogeneities arising from the release of latent heat [22]. These considerations, while interesting and important, are not investigated in this work. The dynamics of the bubble we obtain here come from the simplified description of the field subject to a potential interacting with the heat bath by equation 13.

IV. NUMERICAL RESULTS

Equation 13 behaves in a manner consistent with expectations in the basic case of equilibrium thermodynamics. Computational grid step sizes have been found that reproduce behavior present in specific aspects of nucleation. Our investigation into the effects of a thermal bath on the shape and velocity of an expanding bubble wall may now begin.

For the field to be trapped in the metastable state and eventually decay by bubble nucleation to the global vac-

uum, $\tilde{\alpha} > \sqrt{\frac{9}{2}}$. As shown in figure 2, the bubble is created from the background field fluctuations. Eventually the fluctuations are large enough to form a critical bubble, a bubble that is large enough to complete the phase transition and grow. To distinguish bubble formation from spurious background fluctuations computationally, we examine the field searching for values greater than the turning point. Once a segment of length 10 in ρ has been found whose members satisfy this criterion, it is marked as an expanding bubble.

The shape of the bubble wall in figure 2 is reminiscent of the hyperbolic tangent thin-wall configurations. Generalizing equation 10, we obtain

$$\Phi(\rho, f) = \frac{\Phi_+}{2} [1 - \tanh(\rho f)] \quad (14)$$

where Φ_+ is the global minimum and f^{-1} specifies the thickness of the wall. In figure 3a and 3b, equation 14 is used to fit expanding walls generated in baths with $\tilde{\alpha} = 2.8$, $\tilde{\gamma} = 1.0$, $T = 3.0$ and $\tilde{\alpha} = 3.1$, $\tilde{\gamma} = 2.0$, $T = 1.0$ respectively. While the smoothness of the wall is altered when temperature is varied as asymmetry and viscosity remain constant, the bubble wall’s mean shape does not change.

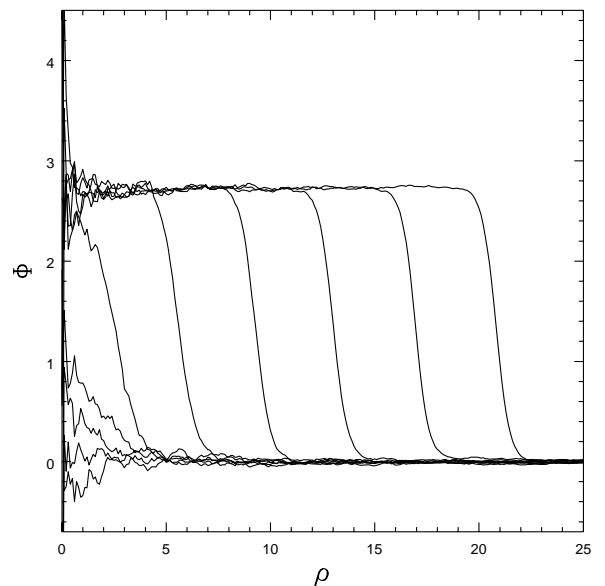


FIG. 2. Snapshots of bubble evolution from the background field. The potential has an asymmetry $\tilde{\alpha} = 3.1$ and the heat bath is characterized by $\tilde{\gamma} = 1.0$ and $T = 1.0$. The interval between snapshots is $\Delta\tau = 10^{-2}$.

Figure 3a

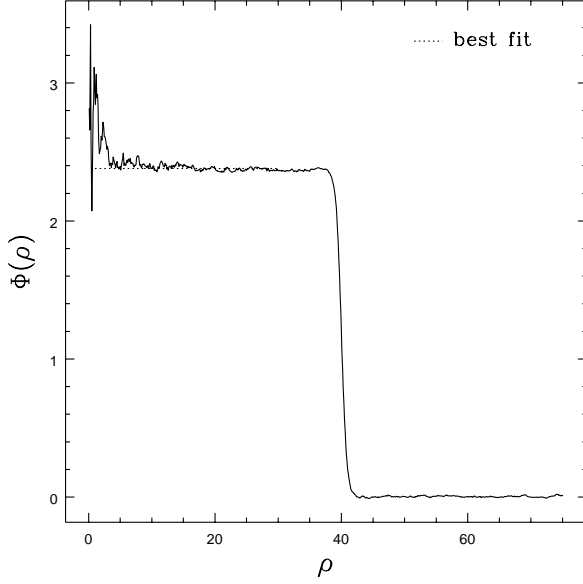


Figure 3b

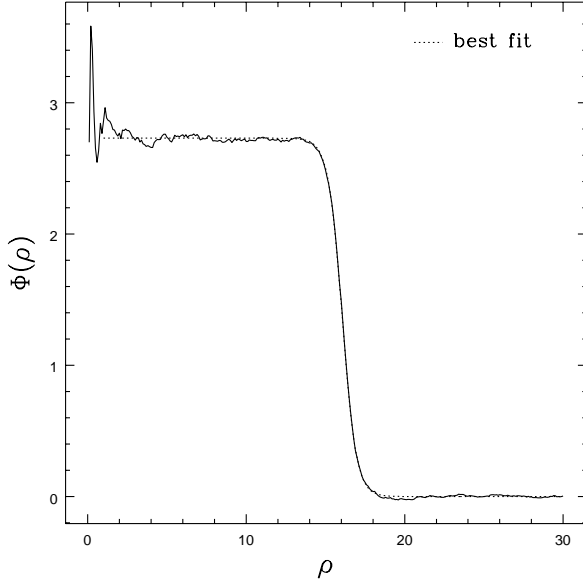


FIG. 3. Snapshots of expanding bubbles with equation providing best fit given by equation 14 for (a) $\tilde{\alpha} = 2.8$, $\tilde{\gamma} = 1.0$, $T = 3.0$ and (b) $\tilde{\alpha} = 3.1$, $\tilde{\gamma} = 2.0$, $T = 1.0$.

The dependence of the wall thickness on the asymmetry of the potential and viscosity of the thermal bath can be found numerically by holding one quantity constant while varying the other. For $\tilde{\gamma} = 1.0$ and $\tilde{\alpha}$ ranging between 2.4 and 3.4, figure 4 shows that the data for f can be described by a linear equation

$$f(\tilde{\alpha}) = A\tilde{\alpha} - B \quad (15)$$

with $A = 1.21$ and $B = 2.20$. In figure 5, the numerical results of f as asymmetry is held constant and viscosity varies is shown to be well fit by the equation

$$f(\tilde{\gamma}) = A\tilde{\gamma}^{-\frac{3}{2}} + B \quad (16)$$

with $A = 0.512$ and $B = 0.969$.

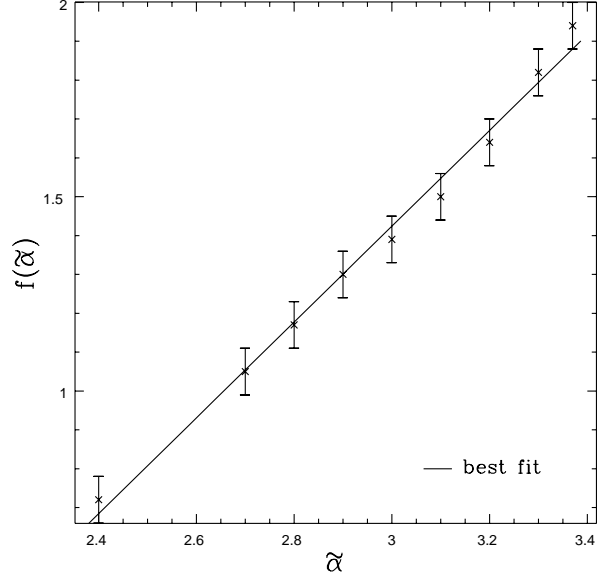


FIG. 4. $f(\tilde{\alpha})$ vs. asymmetry for constant viscosity $\tilde{\gamma} = 1.0$. The equation providing best fit is $A\tilde{\alpha} - B$ where $A = 1.21$ and $B = 2.20$.

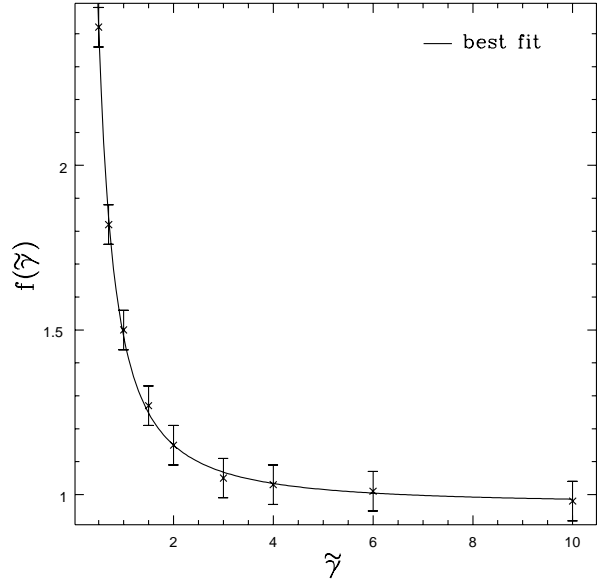


FIG. 5. $f(\tilde{\gamma})$ vs. viscosity for constant asymmetry $\tilde{\alpha} = 3.1$. The equation providing best fit is $A\tilde{\gamma}^{-\frac{3}{2}} + B$ where $A = 0.512$ and $B = 0.969$.

To ascertain the kinematics of the bubble wall, a computational technique for determining the size of the bubble must be developed. As the turning point interpolates between the two vacua, the size of the bubble can be defined as that radial distance which corresponds to the

field configuration value being equal to the turning point. Recording the bubble size at a particular time allows one to find the wall velocity through the equation $v_{bw} = \frac{\Delta \rho}{\Delta \tau}$ where $\Delta \rho$ is the difference between the bubble size at successive times and $\Delta \tau$ is the difference between the corresponding times. In order to limit the already intensive use of computational resources employed in this study, the simulations were terminated once the bubble reached a size of 80. Several trials with longer cutoff sizes were performed and found to yield no additional benefit for the parameters probed.

The development of the bubble wall velocity through time is shown in figure 6. The graph clearly indicates a region in which the bubble wall is accelerating, eventually reaching a terminal velocity. Since the region of acceleration is only of a limited duration, we will ignore this, deferring a detailed analysis of the feature to later studies. Additionally, the restriction imposed of identifying an expanding bubble by a region of true vacuum phase of size 10 (in ρ) and greater in most cases obscures the accelerating wall behavior. Thus, although the data obtained exhibits an acceleration in the start of a bubble's life, our computational methods restrict us to a purely qualitative analysis of this phenomena.

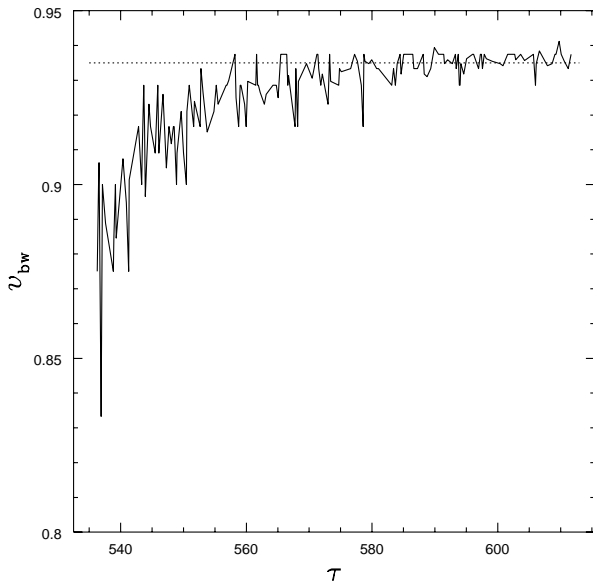


FIG. 6. Bubble wall velocity vs. time for $\tilde{\alpha} = 3.1$, $\tilde{\gamma} = 0.5$, and $T = 0.5$. The dotted line indicates the constant bubble wall velocity 0.935.

The value for the velocity of the bubble wall is determined numerically through use of a “windowing” least squares method. The data over which a least squares fit for a linear equation was performed was adjustable so as to find those portions which had a slope $|\frac{dv_{bw}}{d\rho}| \leq 10^{-5}$. Once this criterion had been satisfied, the intercept was interpreted as the terminal expansion velocity of the bub-

ble. For added certainty, a second method of smoothing the velocity as a function of time data using a Savitzky-Golay type filtering scheme was employed concurrently [23]. By examining the graph, the velocity could be visually discerned. Both methods produced values in agreement with each other.

As in the case of the wall shape, the velocity of the wall was found to be invariant to the temperatures of the bath probed here ($T = 10^{-4}$ to $T = 10$). To insure that this is not an artifact of some statistical dependence in the noise term, all computational simulations were given different random number seeds and a reliable random number generator used [23]. The generator was also checked for any correlations and none were found. The parameters affecting the velocity were the bath viscosity and the potential asymmetry.

The bubble wall terminal velocity's dependence on asymmetry of the potential for constant viscosity $\tilde{\gamma} = 1.0$ is shown in figure 7. The best fit equation to the numerical data is provided by

$$v_{bw}(\tilde{\alpha}) = \frac{1}{1 + A\tilde{\alpha} + B\tilde{\alpha}^2} + 1 \quad (17)$$

with $A = 1.61$ and $B = -1.16$.

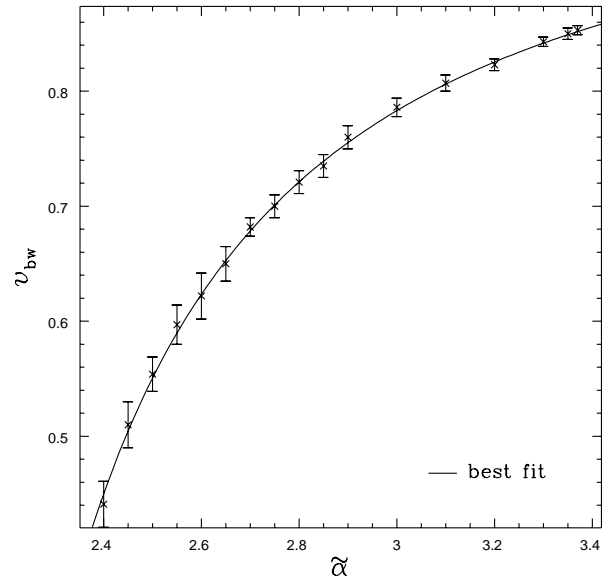


FIG. 7. Bubble wall velocity vs. asymmetry for constant viscosity ($\tilde{\gamma} = 1.0$) and temperature ($T = 1.0$). The equation providing best fit is $\frac{1}{1 + A\tilde{\alpha} + B\tilde{\alpha}^2} + 1$ where $A = 1.61$ and $B = -1.16$.

In figure 8, the asymmetry was fixed to $\tilde{\alpha} = 3.1$ while the viscosity was allowed to vary. The velocity's dependence is well approximated by the expression

$$v_{bw}(\tilde{\gamma}) = \frac{A}{1 + B\tilde{\gamma}^C} + D \quad (18)$$

with $A = 0.949$, $B = 0.275$, $C = 1.62$, and $D = 0.0584$.

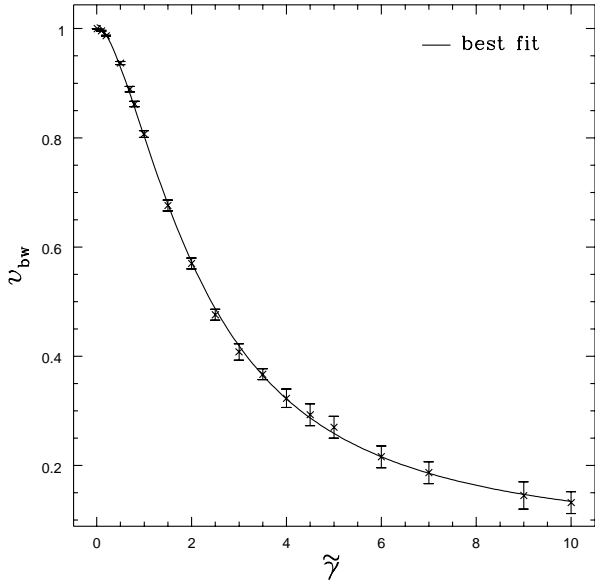


FIG. 8. Bubble wall velocity vs. viscosity for constant asymmetry ($\tilde{\alpha} = 3.1$) and temperature ($T = 1.0$). The equation providing best fit is $\frac{A}{1+B\tilde{\gamma}^C} + D$ where $A = 0.949$, $B = 0.275$, $C = 1.62$, and $D = 0.0584$.

V. CONCLUSIONS

We investigated the shape and velocity of expanding bubble walls in the presence of a thermal bath. The dynamics of the system were modeled by a generalized Langevin equation with a Markovian bath and an asymmetric double well potential. The bubbles were generated naturally from the background thermal field without need for specifying an initial configuration. In the absence of the thermal bath, expanding bubbles eventually reach a terminal velocity of the speed of light and, in the thin wall limit, will have a profile corresponding to a hyperbolic tangent shape.

The presence of a thermal background strongly affects the shape and velocity of the wall. While the relevant aspects of the system were invariant under changing temperatures, asymmetry and viscosity altered the dynamics of the expanding bubbles. The shape of the wall is well approximated by the thin wall shape with a thickness parameter that is dependent on both viscosity and asymmetry. The inverse thickness of the bubble for changing asymmetries is given by equation 15. In the presence of a heat bath, as the asymmetry increases, the thickness of the bubble wall decreases. For changing viscosity, the shape is given by equation 16. The thickness of the bubble wall is found to increase as the viscosity increases. Unlike the expected results of increasing wall thickness as asymmetry grows for no thermal background [11], the results here indicate that a relationship exists between viscosity which thickens bubbles and increasing asymme-

try which tends to entice the system back to the expected results. For velocity, the dependence on asymmetry is approximated by equation 17. As the asymmetry of the potential increases in the presence of a heat bath, the velocity will approach the expected value of unity, the speed of light. Yet, as is shown by equation 18, the viscosity slows the bubble wall. Here the equation behaves as expected in the limit $\tilde{\gamma} \rightarrow 0$ giving light speed velocities for the expanding bubble wall. If equation 18 is carried to large viscosity, the unsettling behaviour of velocities for all viscosities exists. In fact, letting $\tilde{\gamma} \rightarrow \infty$ one finds a suggestive lower bound on expansion speeds of 0.0584. This would indicate that viscosity alone can never prevent the bubble from growing. Yet, taking this result too seriously may lead to error due to the lack of numerical trials of sufficiently large viscosities performed and the methodology employed. It must be borne in mind that our investigation has focused on only growing bubbles which evolve naturally from the false vacuum. For large viscosities, the possibility of finding well-defined, expanding bubbles becomes questionable. This possibility in turn may lead to a discontinuity in an extended investigation of velocity vs. time, eventually leading to the expected result of zero velocity.

Our investigation focused on spherically symmetric solutions to a Langevin equation with a Markovian bath. Yet, there remain several questions whose answers would provide much new information on the subject of first order phase transitions. To model truly real-world phenomena, ideally one would employ a fully dimensional equation of motion. The prospects of doing this present serious challenges not only in the amount of present-day computational resources needed but also in such concepts as clearly defining a bubble wall velocity. An interesting extension of this study appears to be in the determination of the acceleration of the walls from bubble creation to the time of terminal velocity seen in the first few moments of figure 6. More fundamental to the investigation of interacting field theories, it is possible that the thermal background will furnish more complicated properties such as non-additive couplings and/or nonlocal correlations in time and space [19]. The consequences of these nonlocal effects are still questionable, but it is clear that their inclusion into the dynamics of the system by coupling to more general thermal baths may have very significant effects on the shape and speed of the bubble walls. Of more fundamental theoretical importance is the possible connection between the electroweak phase transition and the evolution of the system according to the Langevin equation. While the methods employed here are strongly suggestive of the electroweak phase transition, the work of proving the connection between the two is left as an open question.

ACKNOWLEDGMENTS

I would like to thank James Fry and Marcelo Gleiser for many useful discussions. Additionally, I would like to thank John Yelton and the high energy experimental group at the University of Florida for access to many computer resources. This work was also supported in part by the University of Florida and the IBM Corporation through their Research Computing Initiative at the Northeast Regional Data Center.

-
- [1] M. Gleiser, E. Kolb, and R. Watkins, Nucl. Phys. **B364**, 411 (1991); N. Tetradis, Z. Phys. **C57**, 331 (1993); J. Borrill and M. Gleiser, Phys. Rev. **D51**, 4111 (1995); T. Shiromizu, M. Morikawa, and J. Yokoyama, Prog. Theor. Phys. **94**, 805 (1995); T. Uesugi, M. Morikawa, and T. Shiromizu, Prog. Theor. Phys. **96**, 377 (1996);
 - [2] I. L. Bogolubsky and V. G. Makhankov, Pis'ma Zh. Eksp. Teor. Fiz. **24**, 15 (1976) [JETP Lett., **24**, 12 (1976)]; *ibid.* **25**, 120 (1977) [*ibid.* **25**, 107 (1977)]; V. G. Makhankov, Phys. Rep. **C 35**, 1 (1978); M. Gleiser, Phys. Rev. **D49**, 2978 (1994); E.J. Copeland, M. Gleiser, and H.-R. Müller, Phys. Rev. **D52**, 1920 (1995).
 - [3] M. Gleiser and R. Haas, Phys. Rev. **D54**, 1626 (1996).
 - [4] K. Enqvist, J. Ignatius, K. Kajantie, and K. Rummukainen, Phys. Rev. **D45**, 3415 (1992); B. Liu, L. McLerran, and N. Turok, Phys. Rev. **D46**, 2668 (1992).
 - [5] M. Abney, Phys. Rev. **D55**, 582 (1997).
 - [6] A. Guth, Phys. Rev. **D23**, 347 (1981); A. Linde, Phys. Lett. **108B**, 389 (1982); A. Albrecht and P. Steinhardt, Phys. Rev. Lett. **48**, 1220 (1982).
 - [7] V. Kuzmin, V. Rubakov, and M. Shaposhnikov, Phys. Lett. **155B**, 36 (1985); P. Arnold and L. McLerran, Phys. Rev. **D36**, 581 (1987); N. Turok and J. Zadrozny, Phys. Rev. Lett. **65**, 2331 (1990); M. Dine, R. Leigh, P. Huet, A. Linde, and D. Linde, Phys. Rev. **D46**, 550 (1992); T. Prokopec, R. Brandenberger, and A. Davis, BROWN-HET-1029, CLNS 95/1383, DAMTP 95-73, hep-ph/9601327.
 - [8] E. Witten, Phys. Rev. **D30**, 272 (1984); J. Appelgate and C. Hogan, Phys. Rev. **D31**, 3037 (1985).
 - [9] K. Kirzhnits and A. Linde, Ann. Phys. **101**, 195 (1976).
 - [10] A. Sakharov, JETP Letters **5**, 24 (1967).
 - [11] E. Kolb and M. Turner, *The Early Universe* (Addison-Wesley, 1990).
 - [12] S. Coleman, Phys. Rev. **D15**, 2929 (1977); C. Callan and S. Coleman, Phys. Rev. **D16**, 1762 (1977).
 - [13] A. Linde, Nucl. Phys. **B216**, 421 (1983) [erratum: **223**, 544 (1983)].
 - [14] P. Ramond, *Field Theory: A Modern Primer 2nd edition* (Addison-Wesley, 1989).
 - [15] G. Anderson, Phys. Lett. **B295**, 32 (1992); K. Enqvist, A. Riotto, and I. Vilja, Phys. Rev. **D52**, 5556 (1995).
 - [16] M. Alford, H. Feldman, and M. Gleiser, Phys. Rev. Lett. **68**, 1645 (1992); M. Alford, H. Feldman, and M. Gleiser, Phys. Rev. **D47** 2168 (1993); F.J. Alexander and S. Habib, Phys. Rev. Lett. **71**, 955 (1993).
 - [17] O. Valls and G. Mazenko, Phys. Rev. **B42**, 6614 (1990); M. Alford and M. Gleiser, Phys. Rev. **D48**, 2838 (1993).
 - [18] D. Kirzhnits, JETP Lett. **15**, 529 (1972); D. Kirzhnits and A. Linde, Phys. Lett. **42B** 471 (1972); G. Anderson and L. Hall, Phys. Rev. **D45** 2685 (1992).
 - [19] S. Jeon, Phys. Rev. **D47**, 4586 (1993); M. Gleiser and R. Ramos, Phys. Rev. **D50**, 2441 (1994).
 - [20] H. Kurki-Suonio and M. Laine, Phys. Rev. Lett. **77**, 3951 (1996); H. Kurki-Suonio and M. Laine, Phys. Rev. **D54**, 7163 (1996).
 - [21] M. Kamionkowski and K. Freese, Phys. Rev. Lett. **69**, 2743 (1992); P. Huet, K. Kajantie, R. Leigh, B.H. Liu, and L. McLerran, Phys. Rev. **D48**, 2477 (1993); M. Abney, Phys. Rev. **D49**, 1777 (1994).
 - [22] G.D. Moore and T. Prokopec, Phys. Rev. **D52**, 7182 (1995); A. Heckler, Phys. Rev. **D51**, 405 (1995).
 - [23] W.H. Press et al. *Numerical Recipes* (Cambridge University Press, Cambridge, UK, 1986).